Indian Journal of Science and Technology, *Vol 9(48), DOI: 10.17485/ijst/2016/v9i48/97772, December 2016*
ISSN (Print) : 0974-6846
ISSN (Online) : 0974-5645

Flow and Heat Transfer Towards a Stretching Surface in a Rotating Nanofluid with Suction

Siti Nur Alwani Salleh, Norfifah Bachok and Norihan Md. Arifin

Department of Mathematics and Institute for Mathematical Research, Universiti Putra Malaysia, UPM, Serdang - 43400, Selangor, Malaysia

Abstract

This numerical study is concerned with the rotating boundary layer flow past a stretching surface with the presence of suction in a water-based nanofluid. There are three types of nanoparticles that we consider in this study, namely copper Cu, alumina Al_2O_3 and titania TiO_2. Similarity transformations are used to transform the governing equations corresponding to the momentum and energy equations in the form of partial differential equations into nonlinear ordinary differential equations. Later, these ordinary differential equations are solved numerically by using a shooting method which implemented in Maple software. The results for the skin friction coefficients, local Nusselt number, velocity and the temperature profiles are graphically presented through graphs for various values of the physical parameters of interest, namely rotation, suction and nanoparticle volume fraction parameters. It is revealed from the study that the presence of the suction at the boundary widen the range for which the solutions exist.

Keywords: Dual Solutions, Heat Transfer, Nanofluid, Rotating Flow, Stretching Surface

1. Introduction

Since the past few years, the consideration of the rotating boundary layer flow and heat transfer induced by a stretching surface have received much attention in technological and industrial processes due to its important appearance of cooling and heating process. Several familiar applications are hot rolling, cooling and drying of paper, aerodynamic extrusion of plastic sheets and so on. Sakiadis[1] was the first author who performed the numerical study involving the flow over a continuous moving surface. Since then, various aspects of the flow due to a stretching surface can be noticed in the literature. For instance, Crane[2] studied the boundary layer flow past a stretching plate and the idea later was extended by Gupta and Gupta[3] to the heat and mass transfer due to a stretching sheet which subject to suction and blowing.

The works regarding the flow of a rotating fluid are in continuously growing and have gained more interest in several aspects by some authors like Wang[4], Rajeswari and Nath[5], and Nazar et al.[6] involving a stretching surface. Other than that, the study of the flow of power-law fluid has been considered by Kumari et al[7]. The above mentioned works later were continued by Takhar et al.[8], Abbas et al.[9] and Mahmood et al.[10] towards a stretching sheet with the presence of magnetic field. In recent years, the problems regarding MHD rotating boundary layer flow past a stretched surface have become more important in astrophysics and geophysics, the structure of rotating magnetic stars and also the development of the sunspot which presented by Dieke[11]. Besides, the rotating viscous flow over a shrinking sheet with the presence of suction is discussed by Ali et al[12]. The study proved that in order to maintain the flow due to a shrinking sheet, the mass

*Author for correspondence

suction is required. Other than that, the problems involving the MHD rotating flow past a shrinking surface have been analyzed by Hayat et al.[13], Sajid et al.[14] and Faraz and Khan[15].

However, the above problems have not dealt with the nanofluid yet. Nadeem et al.[16] was among the first who considered the rotating nanofluid due to a stretching surface. A few decade ago, Choi[17] was discovered the uses of the nanofluid and has introduced it to the real world applications. From the study, he noticed that the summation of a small quantity ($<1\%$ volume fraction) of nanoparticles to convectional heat transfer fluid enhanced the thermal conductivity of the fluid twice. Nevertheless, the convectional heat transfer fluid like water, mineral oils and ethylene glycol has low thermal conductivity and may be inadequate to achieve the qualification of the cooling rate. To improve the heat transfer of such fluids, an alternative way is used by dispersing the nanoparticles in a base fluid to form a nanofluid. Nanofluid can be defined as the fluid which contained nanometer-sized particles called nanoparticles. This fluid has no additional problems like sedimentation, additional pressure drop, erosion as well as non-Newtonian behavior. The reason is due to the tiny size and the lower nanoparticle volume fraction needed for the conductivity enhancement. Nowadays, nanofluid has gained a huge number of interests in research area as they are widely used in engineering and biomedical area such as in heat exchangers, electronic cooling, nano drug delivery and the cooling of an automotive application as well. Some studies relate with the flow of a nanofluid over a stretched surface are considered by Khan and Pop[18], Makinde and Aziz[19], Bachok et al.[20] and many others.

Since less works regarding rotating flow of a nanofluid have been reported in literature, hence present work is carried out to analyze the rotating flow due to a stretched surface in a nanofluid with the presence of mass suction. In contrast to Nadeem et al.[16], present study deals with the mass suction at the boundary. The resulting system of ordinary differential equations corresponding to the momentum and energy equations are solved numerically using a shooting method in Maple software. The Prandtl number is taken as $\mathrm{Pr}=6.2$ (water).

2. Basic Equations

Here we consider a steady laminar boundary layer flow of an incompressible water based nanofluid and heat transfer towards a stretching surface at $z=0$. The velocity components along x, y and z directions are assumed to be u, v and w, respectively. The fluid is rotating with a constant angular velocity Ω in the z direction. Based on the above assumptions, the equations that govern the rotating flow and heat transfer can be expressed as follow

$$\frac{\partial u}{\partial x}+\frac{\partial v}{\partial y}+\frac{\partial w}{\partial z}=0, \tag{1}$$

$$u\frac{\partial u}{\partial x}+v\frac{\partial u}{\partial y}+w\frac{\partial u}{\partial z}-2\Omega v=\frac{\mu_{nf}}{\rho_{nf}}\left(\frac{\partial^2 u}{\partial z^2}\right), \tag{2}$$

$$u\frac{\partial v}{\partial x}+v\frac{\partial v}{\partial y}+w\frac{\partial v}{\partial z}+2\Omega u=\frac{\mu_{nf}}{\rho_{nf}}\left(\frac{\partial^2 v}{\partial z^2}\right), \tag{3}$$

$$u\frac{\partial T}{\partial x}+v\frac{\partial T}{\partial y}+w\frac{\partial T}{\partial z}=\alpha_{nf}\left(\frac{\partial^2 T}{\partial z^2}\right), \tag{4}$$

The boundary conditions associated with the above flow are

$$\begin{aligned} &u=ax,\ v=0,\ w=-w_0,\ T=T_w \text{ at } z=0,\\ &u\to 0,\ v\to 0,\ T\to T_\infty \text{ as } z\to\infty \end{aligned} \tag{5}$$

where a is a positive value which represents a stretching constant. The temperature of the fluid is assumed as T, T_w is wall temperature and T_∞ is ambient temperature. Besides, w_0 is a constant mass flux in which $w_0<0$ for suction and $w_0>0$ for injection. The dynamic viscosity, density, thermal diffusivity and the thermal conductivity of the nanofluid, respectively, are given as μ_{nf}, ρ_{nf}, α_{nf} and k_{nf}. While, k_f is the thermal conductivity of the base fluid. All these parameters relate to the nanoparticle volume fraction φ are as follows

$$\rho_{nf}=\rho_f\left[1-\varphi+\varphi\left(\frac{\rho_s}{\rho_f}\right)\right],\ \mu_{nf}=\frac{\mu_f}{(1-\varphi)^{2.5}},\ \alpha_{nf}=\frac{k_{nf}}{\left(\rho C_\rho\right)_{nf}},$$

$$\left(\rho C_\rho\right)_{nf}=\left(\rho C_\rho\right)_f\left[1-\varphi+\varphi\frac{\left(\rho C_\rho\right)_s}{\left(\rho C_\rho\right)_f}\right],\ \frac{k_{nf}}{k_f}=\frac{k_s+2k_f-2\varphi\left(k_f-k_s\right)}{k_s+2k_f+\varphi\left(k_f-k_s\right)} \tag{6}$$

In which the volumetric heat capacities of solid nanoparticle, base fluid, and nanofluid are assumed as $\left(\rho C_\rho\right)_s$, $\left(\rho C_\rho\right)_f$ and $\left(\rho C_\rho\right)_{nf}$ respectively. Besides, k_s

is thermal conductivity of solid nanoparticle, ρ_f and μ_f are the density and dynamic viscosity of the base fluid, respectively.

Now we introduce the following similarity transformations

$$u = axf'(\eta),\ v = axh(\eta),\ w = -\sqrt{a\nu}f(\eta),$$

$$\eta = z\sqrt{\frac{a}{\nu}},\ \theta(\eta) = \frac{T - T_\infty}{T_w - T_\infty} \tag{7}$$

By using the Eqs. (6) and (7), Eq. (1) is satisfied and Eqs. (2) – (4) become the following ordinary differential equations as shown below

$$\frac{1}{(1-\varphi)^{2.5}\left[1-\varphi+\varphi\left(\rho_s/\rho_f\right)\right]}f'''+ff''-f'^2+2\Omega h = 0, \tag{8}$$

$$\frac{1}{(1-\varphi)^{2.5}\left[1-\varphi+\varphi\left(\rho_s/\rho_f\right)\right]}h''+fh'-f'h-2\Omega f' = 0, \tag{9}$$

$$\frac{1}{\Pr\left[1-\varphi+\varphi\left(\rho C_\rho\right)_s/\left(\rho C_\rho\right)_f\right]}\theta''+f\theta' = 0. \tag{10}$$

subjected to the boundary conditions (5) which become

$$f(0) = s,\ f'(0) = 1,\ h(0) = 0,\ \theta(0) = 1,$$
$$f'(\eta)\to 0,\ h(\eta)\to 0,\ \theta(\eta)\to 0 \text{ as } \eta\to\infty \tag{11}$$

where $\Pr = \nu_f/\alpha_f$ is the Prandtl number. The rotation parameter is $\Omega = \overline{\Omega}/a$ and the constant mass flux parameter is given as s in which $s > 0$ for suction and $s < 0$ for injection.

The local skin friction coefficients of x and y components as well as the local Nusselt number can be defined as

$$Cf_x = \frac{\tau_{xz}}{\rho_f(ax)^2},\ Cf_y = \frac{\tau_{yz}}{\rho_f(ax)^2},\ Nu_x = \frac{xq_w}{k_f(T_w - T_\infty)} \tag{12}$$

where shear stresses along x and y components are τ_{xz} and τ_{yz}, respectively and heat flux q_w are given by

$$\tau_{xz} = \mu_{nf}\left(\frac{\partial u}{\partial z}\right)_{z=0},\ \tau_{yz} = \mu_{nf}\left(\frac{\partial v}{\partial z}\right)_{z=0},\ q_w = -k_{nf}\left(\frac{\partial T}{\partial z}\right)_{z=0} \tag{13}$$

Replace Eq. (13) into Eq. (12), we will obtain

$$Cf_x(\mathrm{Re}_x)^{\frac{1}{2}} = \frac{1}{(1-\varphi)^{2.5}}f''(0),\ Cf_y(\mathrm{Re}_x)^{\frac{1}{2}} = \frac{1}{(1-\varphi)^{2.5}}h'(0),$$
$$Nu_x(\mathrm{Re}_x)^{-\frac{1}{2}} = -\frac{k_{nf}}{k_f}\theta'(0). \tag{14}$$

Table 1. Thermophysical properties of base fluid and nanoparticles (Oztop and Abu-Nada[21]).

Physical properties	Fluid phase (water)	Cu	Al_2O_3	TiO_2
C_p (J/kg K)	4179	385	765	686.2
ρ (kg/m^3)	997.1	8933	3970	4250
k (W/mK)	0.613	400	40	8.9538

3. Results and Discussion

The resulting system of ordinary differential equations (8) – (10) associated with the conditions (11) are solved numerically using a shooting method with the help of Maple software. Through this method, the various initial guesses for the unknown values of $f''(0)$, $h'(0)$ and $-\theta'(0)$ are set in which all the profiles have to satisfy the conditions (11) asymptotically with the different shapes. In this study, three different types of nanoparticles namely, Cu, Al_2O_3 and TiO_2 are considered as the working fluid. The Prandtl number is taken as $\Pr = 6.2$ which represents water. In order to assess the accuracy of the current method, the comparison has been made with the case of non-permeable surface $(s = 0)$ for numerical values of $Cf_x(\mathrm{Re}_x)^{1/2}$, $Cf_y(\mathrm{Re}_x)^{1/2}$ and $Nu_x(\mathrm{Re}_x)^{-1/2}$ studied by Nadeem et al[16]. The comparison values can be seen in Table 2 – 4 and it is found in excellent agreement between the two sets of data. From the table, we can conclude that the skin friction coefficients and the local Nusselt number have higher values for Cu than for Al_2O_3 and TiO_2. These

factor is due to the physical properties of the fluid and nanoparticles shown in Table 1 in which Cu have the higher values of thermal conductivity compared to Al_2O_3 and TiO_2.

Table 2. Comparison for numerical values of $Cf_x(\mathrm{Re}_x)^{1/2}$ when $s = 0$

Nanoparticles	φ	Ω	Nadeem et al[16]	Present result
Cu	0.0	0	1.000000	1.000000
		0.5	1.138381	1.138381
		1	1.325029	1.325029
		2	1.652352	1.652352
	0.1	0	1.528754	1.528754
		0.5	1.740304	1.740307
		1	2.025644	2.025646
		2	2.526040	2.526039
	0.2	0	2.127835	2.127835
		0.5	2.422286	2.422289
		1	2.819443	2.819444
		2	3.515932	3.515932
TiO_2	0.0	0	1.000000	1.000000
		0.5	1.138381	1.138381
		1	1.325029	1.325029
		2	1.652352	1.652352
	0.1	0	1.313734	1.313734
		0.5	1.495529	1.495528
		1	1.740735	1.740735
		2	2.170750	2.170729
	0.2	0	1.699044	1.706218
		0.5	1.934159	1.934159
		1	2.251282	2.251287
		2	2.807419	2.807429
Al_2O_3	0.0	0	-	1.000000
		0.5	-	1.138381
		1	-	1.325029
		2	-	1.652352
	0.1	0	-	1.299751
		0.5	-	1.479611
		1	-	1.722208
		2	-	2.147646
	0.2	0	-	1.702057
		0.5	-	1.901005
		1	-	2.212570
		2	-	2.759201

Figures 1 - 2 show the effects of the nanoparticle volume fraction φ on the variations of $f''(0)$ and $-\theta'(0)$ with suction parameter s for Cu water when $\Omega = 0.0001$. It is observed that as the values of φ increase, the reduced skin friction $f''(0)$ and local heat flux $-\theta'(0)$ are found to decrease. From these graph, we can conclude that dual solutions only exist for $s \geq 0$. In fact,the inclusion of the nanoparticles in the fluid flow is to enhance the heat transfer. Nevertheless, the graphs displayed in Fig. 2 shows that increase the values of φ have reduced the heat transfer rate at the stretched surface.

Figures 3 - 4 display the variations of $f''(0)$ and $-\theta'(0)$ versus s for Cu water when $\varphi = 0.1$ for various values of the rotation parameter Ω. The figures indicate that the values of $f''(0)$ and $-\theta'(0)$ are seem to decrease with an increment values of Ω. It is noticed that when the values of Ω is small enough $(\Omega = 0.0001)$, the dual solutions are found to exist for $s \geq 0$. While beyond this limitation no solutions exist.

The variations of the skin friction coefficients $Cf_x(\mathrm{Re}_x)^{1/2}$, $Cf_y(\mathrm{Re}_x)^{1/2}$ and the local Nusselt number $Nu_x(\mathrm{Re}_x)^{-1/2}$ which given by Eq. (14) for various values of Ω and for different nanoparticles versus φ are illustrated in Figs. 5 - 7 for $s = 2.0$. The absolute values of the skin friction coefficients for both x and y components are seem to increase respectively, for Al_2O_3, TiO_2 and Cu as the rotation Ω and φ increases and these can be found in Figs. 5 - 6. The acceleration of the fluid motion because of the presence of rotation in the fluid flow has reduced the momentum boundary layer thickness. This phenomenon is occurred due to the collision between the nanoparticles and the base fluid particles. Some kinds of behavior will increase the shear stress at the surface as well as the skin friction coefficients. Other than that Fig. 7 shows that increase the Ω results in decrease the local Nusselt number for TiO_2, Al_2O_3 followed by Cu respectively and this quantity decrease linearly with φ. The fact that TiO_2 has the lowest thermal conductivity than Al_2O_3 and Cu which can be proved through Table 1. The presence of the suction in the flow strongly affected the heat transfer rate at the surface.

Table 3. Comparison for numerical values of $Cf_y(\mathrm{Re}_x)^{1/2}$ when $s = 0$

Nanoparticle	φ	Ω	Nadeem et al[17]	Present result
Cu	0.0	0	0.000000	0.000000
		0.5	0.512760	0.837098
		1	0.837098	0.837098
		2	1.287259	1.287259
	0.1	0	0.000000	0.000000
		0.5	0.783884	0.783785
		1	1.279718	1.279718
		2	1.967903	1.967902
	0.2	0	0.000000	0.000000
		0.5	1.091069	1.090941
		1	1.781207	1.781226
		2	2.739074	2.739075
TiO_2	0.0	0	0.000000	0.000000
		0.5	0.512760	0.512760
		1	0.837098	0.837098
		2	1.287259	1.287259
	0.1	0	0.000000	0.000000
		0.5	0.673630	0.673630
		1	1.099724	1.099724
		2	1.691115	1.691155
	0.2	0	0.000000	0.000000
		0.5	0.871202	0.871204
		1	1.422267	1.422275
		2	2.187109	2.187131
Al_2O_3	0.0	0	-	0.000000
		0.5	-	0.512760
		1	-	0.837098
		2	-	1.287259
	0.1	0	-	0.000000
		0.5	-	0.666461
		1	-	1.088019
		2	-	1.673116
	0.2	0	-	0.000000
		0.5	-	0.856271
		1	-	1.397703
		2	-	2.149667

The sample velocities and the temperature profiles are given in Figs. 8 - 16 for various values of rotation, nanoparticles and suction. Figures 8 - 10 show that the velocities of x and y components $f'(\eta)$ and $h(\eta)$ are noticed to decrease when the Ω increases, while the reverse effects occur for the temperature profiles. It is observed from Fig. 10 that the momentum boundary layer thickness undergo reduction due to the acceleration of the fluid motion. The influence of the different nanoparticles on the $f'(\eta)$, $h(\eta)$ and $\theta(\eta)$ are shown in Fig. 11 - 13. The values of $f'(\eta)$ and $h(\eta)$ are seem to increase and decrease respectively, for Cu, TiO_2 and Al_2O_3. While, the values of $\theta(\eta)$ is decreased significantly for Cu, Al_2O_3 and TiO_2.

Table 4. Comparison for numerical values of $Nu_x(\mathrm{Re}_x)^{-1/2}$ when $s = 0$

Nanoparticle	φ	Ω	Nadeem et al[17]	Present result
Cu	0.0	0	1.770948	1.770948
		0.5	1.725631	1.725631
		1	1.660286	1.660286
		2	1.533487	1.533487
	0.1	0	1.933636	2.02837
		0.5	0.851932	1.933842
		1	1.733394	1.797336
		2	1.515517	1.552999
	0.2	0	2.117373	2.360705
		0.5	1.996168	2.189845
		1	1.824178	1.964176
		2	1.53417	1.610834
TiO_2	0.0	0	1.770948	1.770948
		0.5	1.725631	1.725631
		1	1.660286	1.660286
		2	1.533487	1.533487
	0.1	0	1.926447	2.004577
		0.5	1.864745	1.935360
		1	1.775176	1.834770
		2	1.603259	1.646569
	0.2	0	2.093007	2.273332
		0.5	2.015334	2.188907
		1	1.902422	2.041547
		2	1.689698	1.786104
Al_2O_3	0.0	0	-	1.770948
		0.5	-	1.725631
		1	-	1.660286
		2	-	1.533487
	0.1	0	-	1.964407
		0.5	-	1.900797
		1	-	1.808442
		2	-	1.631360
	0.2	0	-	2.158311
		0.5	-	2.089210
		1	-	1.969159
		2	-	1.752650

The effects of the suction on the velocities and temperature profiles are presented in Figs. 14 - 16. The velocity profiles of x component $f'(\eta)$ and the temperature profiles $\theta(\eta)$ are decreased as the values of s increase, while the opposite trends is observed for the velocity profiles of

y component $h(\eta)$. As the values of s become higher, the momentum and thermal boundary layer thickness are reduced. From the Figs. 8 -16, it is noticed that all the profiles have satisfied the following boundary conditions (11) asymptotically and these kinds of behaviors will support the accuracy of the numerical results obtained for the current study.

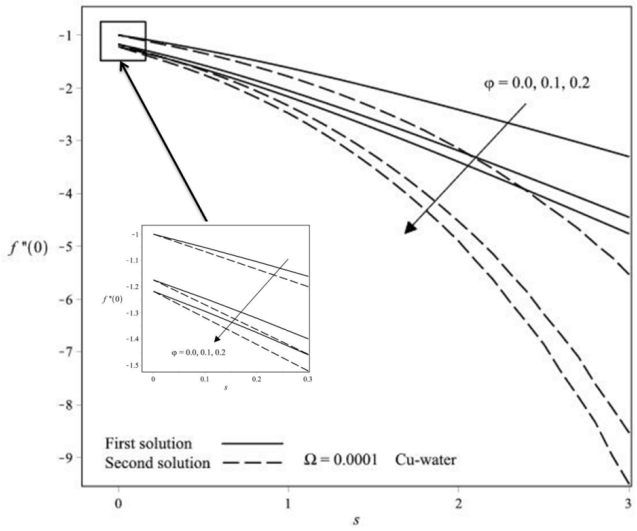

Figure 1. Variations of $f''(0)$ versus s for different values of φ.

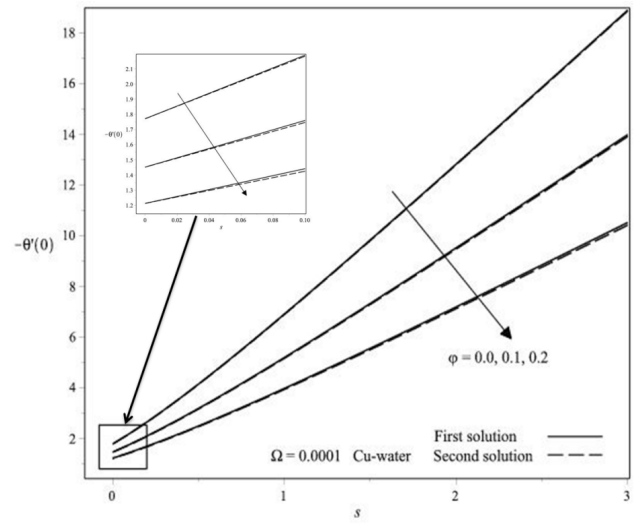

Figure 2. Variations of $-\theta'(0)$ versus s for different values of φ.

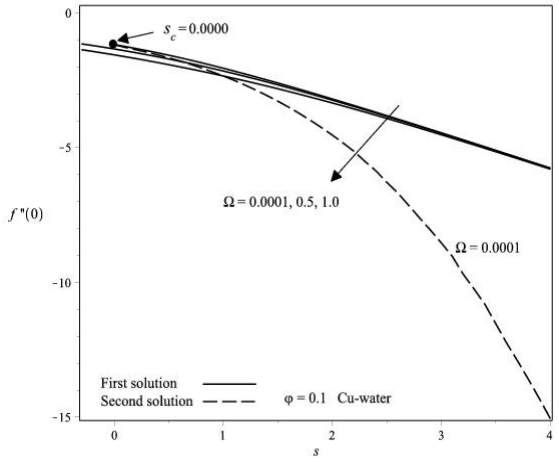

Figure 3. Variations of $f''(0)$ versus s for different values of Ω.

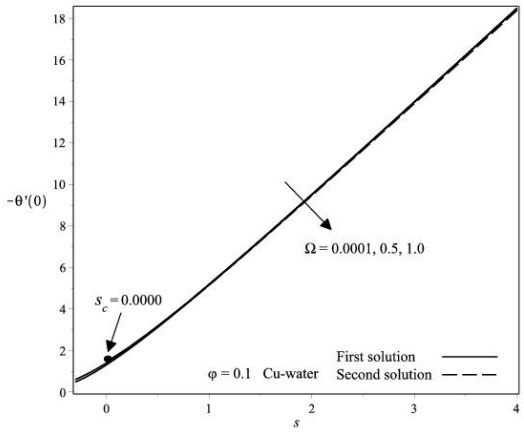

Figure 4. Variations of $-\theta'(0)$ versus s for different values of Ω.

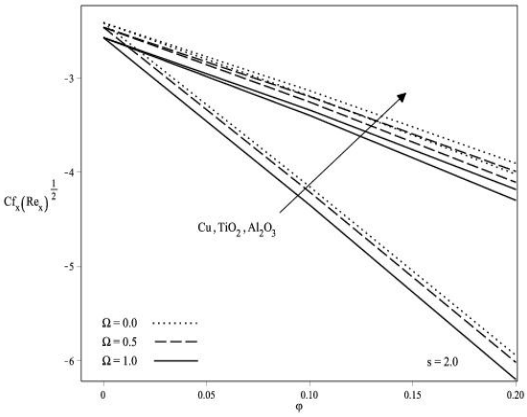

Figure 5. Variations of $Cf_x(\mathrm{Re}_x)^{1/2}$ versus φ for different nanoparticles and Ω.

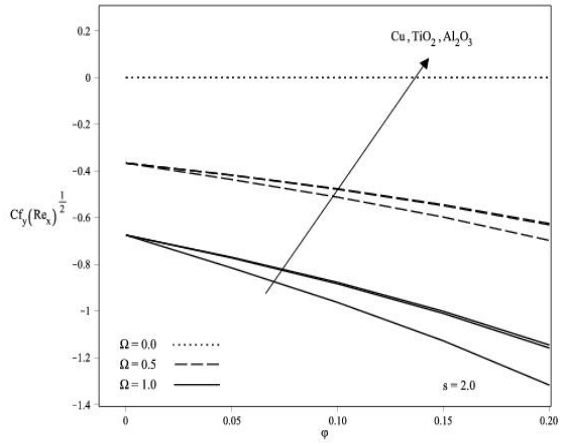

Figure 6. Variations of $Cf_y(\mathrm{Re}_x)^{1/2}$ versus φ for different nanoparticles and Ω.

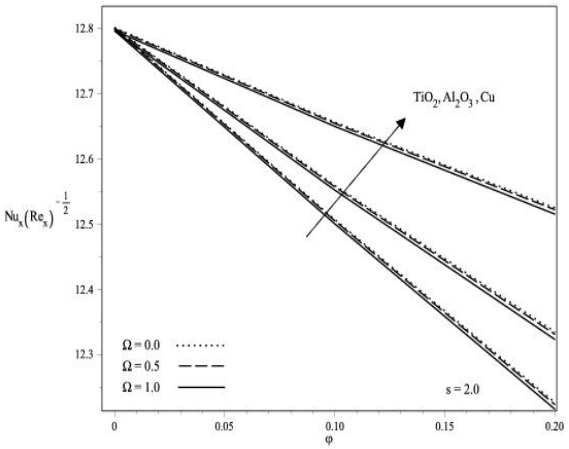

Figure 7. Variations of $Nu_x(\mathrm{Re}_x)^{-1/2}$ versus φ for different nanoparticles and Ω.

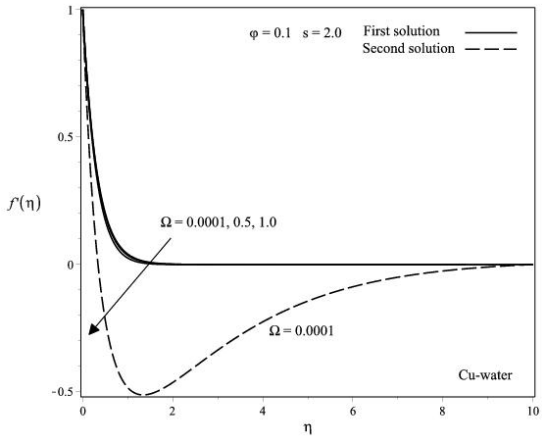

Figure 8. Velocity profiles $f'(\eta)$ for different values of Ω.

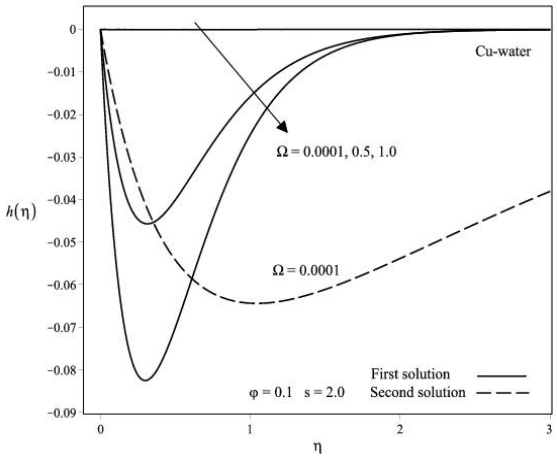

Figure 9. Velocity profiles $h(\eta)$ for different values of Ω.

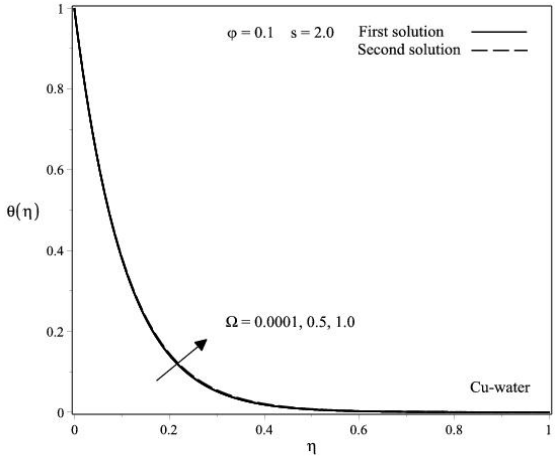

Figure 10. Temperature profiles $\theta(\eta)$ for different values of Ω.

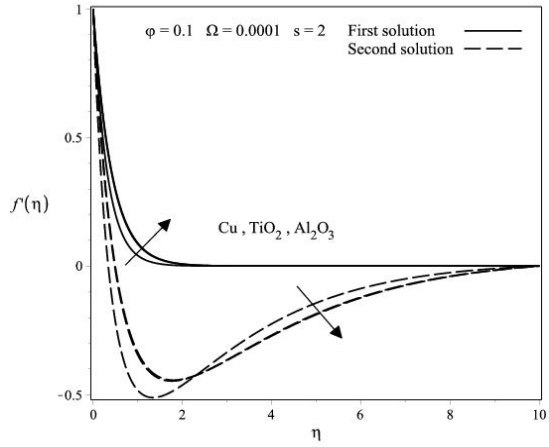

Figure 11. Velocity profiles $f'(\eta)$ for different nanoparticles.

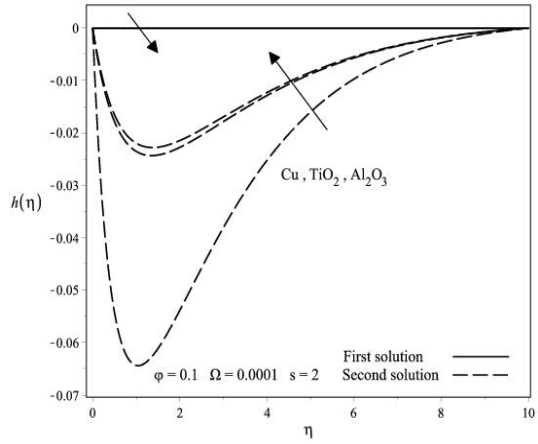

Figure 12. Velocity profiles $h(\eta)$ for different nanoparticles.

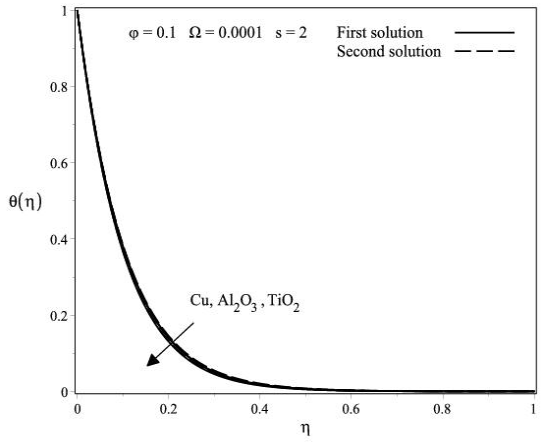

Figure 13. Temperature profiles $\theta(\eta)$ for different nanoparticles.

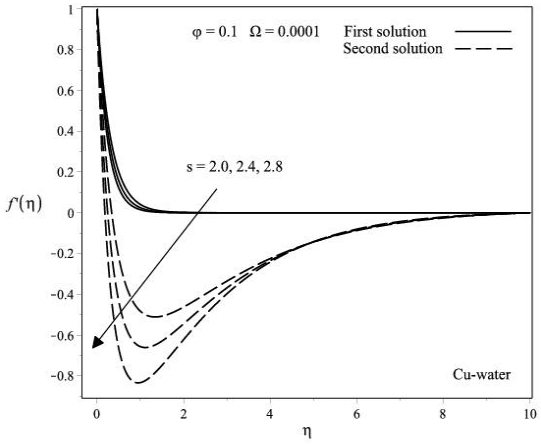

Figure 14. Velocity profiles $f'(\eta)$ for different values of s.

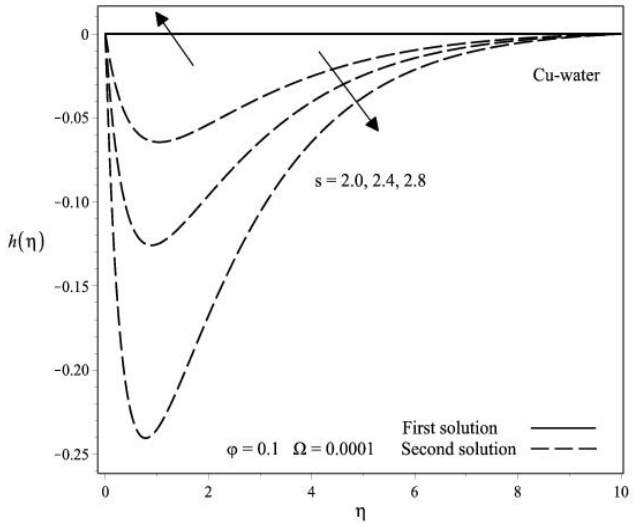

Figure 15. Velocity profiles $h(\eta)$ for different values of s.

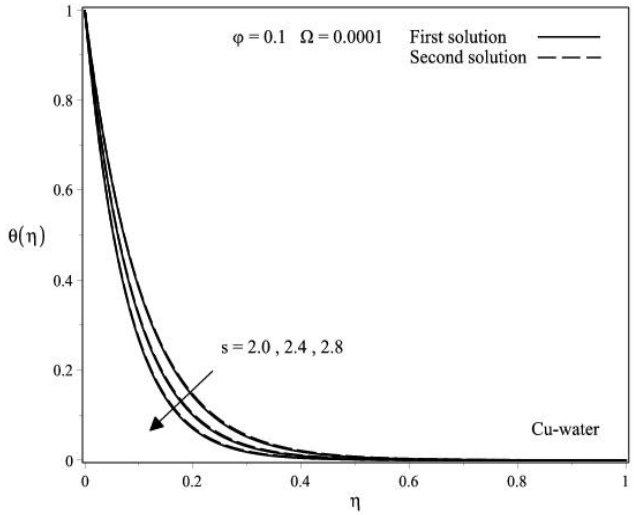

Figure 16. Temperature profiles $\theta(\eta)$ for different values of s.

4. Conclusion

In this problem, the influence of the rotation Ω, nanoparticle volume fraction φ and suction s parameters on the fluid flow and heat transfer characteristics of the rotating nanofluid towards a stretching surface with the presence of mass suction is investigated. The problem has been solved numerically by using a shooting method built in Maple software. From the overall study, we can conclude that

- The absolute values of the skin friction coefficients increase as the rotation and nanoparticle volume fraction parameter increase.
- the local Nusselt number decrease as the values of rotation and nanoparticles volume fraction increase.
- the presence of suction widen the range for which the solution exist and reduced the heat transfer rate at the wall as well.
- the dual solutions are found to exist only when the values of the rotation is small enough and when $s \geq 0$.

5. Acknowledgement

The financial supports received from the ministry of Higher Education, Malaysia (Project code: FRGS/1/2012/SG04/UPM/03/1) and the Research University Grant (RUGS) from the Universiti Putra Malaysia are gratefully acknowledged.

6. References

1. Sakiadis BC. Boundary layer behavior on continuous solid surface. AIChE Journal. 1961; 7:26–8.
2. Crane L. Flow past a stretching plate. Z Angew Math Phys. 1970; 21:445–7.
3. Gupta P, Gupta A. Heat and mass transfer on a stretching sheet with suction and blowing. The Canadian Journal of Chemical Engineering. 1977; 55:744–6.
4. Wang C. Stretching a surface in a rotating fluid. Journal of Applied Mathematics and Physics. 1988; 39:177–85.
5. Rajeswari V, Nath G. Unsteady flow over a stretching surface in a rotating fluid. International Journal of Engineering Science. 1992; 30:747–56.
6. Nazar R, Amin N, Pop I. Unsteady boundary layer flow due to a stretching surface in a rotating fluid. Mechanics Research Communications. 2004; 31:121–8.
7. Kumari M, Grosan T, Pop I. Rotating flow of power-law fluids over a stretching surface. Journal of the Taiwan Institute of Chemical Engineers. 2006; 26:11–9.
8. Takhar H, Chamkha A, Nath G. Flow and heat transfer on a stretching surface in a rotating fluid with a magnetic field. International Journal of Thermal Sciences. 2003; 42:23–31.
9. Abbas Z, Javed T, Ali N. Unsteady MHD flow and heat transfer on a stretching sheet in a rotating fluid. Journal of the Taiwan Institute of Chemical Engineers. 2010; 41: 644–50.
10. Mahmood T, Ali S, Khan M. MHD flow due to a stretching surface in rotating fluid. Journal of Mathematics. 2014; 46:39–50.
11. Dieke RH. Internal Rotation of the Sun. Annual Review of Astronomy and Astrophysics. In: Goldberg L editor. Annual Review Inc. 1997; 8:297.
12. Ali F, Nazar R, Arifin N, Pop I. Unsteady shrinking sheet with mass transfer in a rotating fluid. International Journal7 for Numerical Methods in Fluids. 2010; 66:1465–74.
13. Hayat T, Javed T, Sajid M. Analytic solution for MHD rotating flow of a second grade fluid over a shrinking surface. Physics Letters A. 2008; 372:3264–73.
14. Sajid M, Javed T, Hayat T. Mhd Rotating Flow of a Viscous Fluid over a Shrinking Surface, Nonlinear Dynamics. 2008; 51:259–65.
15. Faraz N, Khan Y. Analytical solution of electrically conducted rotating flow of a second grade fluid over a shrinking surface. Ain Shams Engineering Journal. 2011; 2:221–6.
16. Nadeem S, Rehman A, Mehmood R. Boundary layer flow of rotating two phase nanofluid over a stretching surface. Heat Transfer-Asian Research. 2014; 0:1–14.
17. Choi S. Enhancing thermal conductivity of fluids with nanoparticles. ASME Publication. 1995; 66:99–101.
18. Khan WA, Pop I. Boundary-layer flow of a nanofluid past a stretching sheet. Int Journal of Heat and Mass Transfer. 2010; 53:2477–83.
19. Makinde OD, Aziz A. Boundary layer flow of a nanofluid past a stretching sheet with a convective boundary condition. International Journal of Thermal Sciences. 2011; 50:1326–32.
20. Bachok N, Ishak A, Pop I. Stagnation-point flow over a stretching/shrinking sheet in a nanofluid. Nanoscale Research Letters. 2011; 6:623.
21. Oztop HF, Abu-Nada E. Numerical Study of Natural Convection in Partially Heated Rectangular Enclosures Filled with Nanofluids. International Journal Heat Fluid Flow. 2008; 29:1326–36.